A new waterborne chitosan-based polyurethane hydrogel as a vehicle to transplant bone marrow mesenchymal cells improved wound healing of ulcers in a diabetic rat model

Christian Viezzer[a,b,*], Rafael Mazzuca[d], Denise Cantarelli Machado[d], Maria Madalena de Camargo Forte[a], José Luis Gómez Ribelles[b,c]

[a] *Department of Materials Engineering, Federal University of Rio Grande do Sul, Porto Alegre, RS, Brazil*
[b] *Centre for Biomaterials and Tissue Engineering, Universitat Politècnica de València, 46022 València, Spain*
[c] *Biomedical Networking Research Center on Bioengineering, Biomaterials and Nanomedicine (CIBER-BBN), València, Spain*
[d] *Cellular Therapy Laboratory, Biomedical Research Institute, Pontifical Catholic University of Rio Grande do Sul, Porto Alegre, RS, Brazil*

ARTICLE INFO

ABSTRACT

Foot ulcers, a common complication of diabetes, can cause physical incapacity and are derived from several factors, including poor wound healing. New therapeutic strategies are needed to minimize this complication for the sake of patients' health. We therefore developed a new chitosan- polyurethane hydrogel membrane (HPUC) and the test results confirmed that HPUC present low cytotoxicity and improved wound healing when used with mononuclear bone marrow fraction cells in the diabetic rat model. The biodegradable hydrogels were produced in block copolymer networks with a combination of chitosan blocks and biodegradable polyurethane. The membranes were characterized by FTIR, ^{13}C-NMR and thermogravimetry. Swelling and hydrolytic degradation were also evaluated. The non-solubility of the membranes in good solvents and the chemical characterization confirmed that the network structure was formed between the PU and the chitosan through urea/urethane bonds. The findings confirm that the HPUC have interesting properties that make them suitable for wound healing applications.

1. Introduction

The diabetes mellitus (DM) group of metabolic diseases, whose main characteristic is their hyperglycemic status, can be caused by the lack of insulin, a deficit in the production or reception of this hormone, among other causes. This disease is associated with several complications such as nephropathies, retinopathies, cardiovascular diseases, ulcers and limb amputation. It is a major public health problem worldwide due to its high prevalence and morbidity (Tao, Shi, & Zhao, 2015). Recurrent infections are caused by reduced immunity, a phagocytic function associated with hyperglycemia and poor vascularization (Baltzis, Eleftheriadou, & Veves, 2014; Boulton, 2013; Dinh et al., 2012; Hilfiker, Kasper, Hass, & Haverich, 2011). Cell therapy with bone marrow mesenchymal stem cells has proved to be an effective tissue repair strategy. Although the pathways involved in this repair process have not been fully identified, it is known that transplanted cells release growth factors that modulate the immune response, organize tissues, promote angiogenesis and stimulate cell differentiation. Tissue engineering can aid in the regenerative process by developing new biomaterials that can regenerate wounds, prevent contractions and protect against infectious agents. The tissue repair process occurs in three distinct phases: inflammation, formation and remodeling of new tissue (Baltzis et al., 2014; Boulton, 2013; Dinh et al., 2012; Hilfiker et al., 2011). Besides mitigating the inflammatory process, effective wound healing dressings must have the following characteristics: wound adherence, histocompatibility, fluid loss control and sterility.

In tissue engineering applications, biopolymers are of great interest in the manufacture of three-dimensional supports for cell culture and transplant. Chitosan (CHS) has been shown to be a highly suitable biopolymer for these applications (Tsao et al., 2011; Hilmi et al., 2002; Jiang et al., 2010; Moise et al., 2012). In addition to its good biocompatibility and non-toxicity, CHS has properties of particular interest as a wound-healing dressing, such as antimicrobial activity and excellent hemostatis (Ouyang et al., 2018). However one of its limiting factors is that it is not soluble in most organic solvents, although it can be dissolved in diluted acid solutions, and this hinders its use in the

manufacture of complex structures. Chitosan has reactive amine and hydroxyl side groups occurring in the polymer chains, which can be modified by derivatization (Andrade et al., 2011; Casettari et al., 2012; Merchant et al., 2014). Alkaline treatment has also been used to reduce its molecular weight, if required (Barikani, Honarkar, & Barikani, 2010). These characteristics make it versatile to being modified by grafting specific side groups or complexing with other classes of polymers. Polyurethanes (PUs) synthesized in aqueous dispersion have recently attracted much attention due to their physicochemical properties and biocompatibility (Jiang et al., 2007; Rowlands, Lim, Martin, & Cooper-White, 2007; Wang, Ping, Chen, & Jing, 2006; Zuber, Zia, Mahboob, Hassan, & Bhatti, 2010). The polyester poly (DL lactide-co-glycolide) (PLGA) is the most frequently used polyester in the synthesis of PU-based biomaterials. It has been approved by the FDA for different applications and has been used for many years in the development of medical devices as well as in raw materials for the pharmaceutical industry. Another of its benefits is that its hydrolysis products can be uptaken in the cellular metabolic pathway (Jovanovic et al., 2010; Page et al., 2012).

Bioresorption of CHS takes place by the enzymatic degradation of the polymer chains, although this is a slow process and depends on the location of the implant. Our hypothesis is that combining chitosan in a block copolymer network with other polymers susceptible to hydrolytic degradation will allow fast degradation of the material in aqueous media while maintaining the hydrogel behavior characteristic of chitosan and its proven regeneration capacities. This hypothesis is based on previous works on polymer blends or block copolymers containing chitosan as one of the components (Gámiz-González, Vidaurre, & Gómez Ribelles, 2017; Hu et al., 2012; Ünlü, Pollet, & Avérous, 2018; Cruz, Dunia, Gomez Ribelles, & Salmerón Sánchez, 2008). The novelty of this work was synthesizing PU-chitosan hydrogel membrane (HPUC) by introducing the PLGA blocks into soft PU segments. The hydrogel was formed in two steps, with the reaction of PU prepolymer via aqueous dispersion with unmodified chitosan. In this way, we produced a hydrogel for wound healing by combining CHS and PLGA blocks in a block copolymer network. Thus, we took advantage of PLGA's hydrolysis properties to control degradation. After the physical and chemical characterization of the hydrogel membrane, a biocompatibility test was performed with bone marrow mononuclear cells (BMMNC) before evaluating the membrane combination as a wound-healing dressing and for BMMNC injections in a rat diabetic model. The promising results provided evidence that HPUC plus BMMNC may be used to enhance the wound healing process.

2. Experimental

2.1. Materials

Chitosan [poly-(a-1/4)-2-amino-2-deoxy-D-glucopyranose] was purchased from Sigma-Aldrich with viscosity-average molecular weight of 1500 kDa determined by Mark-Houwink equation using 0.1 M CH_3COOH/0.2 M NaCl as a solvent system at 25 °C and average deacetylation degree (DD) of 75 % determined by first derivative UV spectrophotometry (Cruz, Mercedes, Salmerón-Sánchez, & Gómez-Ribelles, 2012). Hexametylene diisocyanatee (HDI), 2,2- bis(hydroxymethyl) propionic acid (DMPA), Triethylamine (TEA), Tin(II) 2-ethylhexanoate, (3S)-cis-3,6-Dimethyl-1,4-dioxane-2,5-dione (L-Lactide), 1,4-Dioxane-2,5-dione (glycolide) and Streptozocinwere purchased from Sigma-Aldrich. All materials were used as received without further purification.

2.2. Membranes preparation

The hydrogel based on waterborne polyurethane-chitosan (HPUC) was obtained from a polyurethane prepolymer and chitosan. The PU prepolymer was obtained from a polyester diol, previously synthetized,

Sample	NCO/OH 2:1:1			
	PLGAdiol (g)	DMPA/PLGAdiol (wt%)	CS (g)	Swelling Capacity (wt%)
HPUC1	0.25	7	0.75	1200
HPUC2	0.5		0.5	1800
HPUC3	0.75		0.25	2000

HDI and DMPA. Chitosan was used as received.

2.2.1. Synthesis of the polyester diol

The poly(lactid-co-glycolide)diol (PLGAdiol) was synthesized according to Ivirico et al. (2009) (Escobar Ivirico, Salmerón-Sánchez, Gómez Ribelles, & Monleón Pradas, 2009), with some modifications for obtaining a polyester copolymer with Mn of 2000 Da, from a mixture of 50:50 of lactid acid and glycolide. Briefly, for this purpose 0.06 mol of lactide and 0.06 mol of glycolide were reacted with 0.01 mol of ethylene glycol at 120 °C for 4 h at 23 mbar. After synthesis, the polymer was dissolved in acetone, precipitated in hexane under stirring and dried in a vacuum.

2.2.2. Synthesis of the PU prepolymer

All PU prepolymers were obtained at a ratio 2/1/1 of NCO groups in HDI / OH groups in PLGAdiol / OH groups in DMPA with 7 % (wt%) of the internal emulsifier DMPA in relation to the polyester diol. The internal emulsifier was 100 % neutralized with TEA. The amounts of PLGAdiol for each HPUC series are listed in Table 1. The reaction was carried out in a three-necked round bottom flask using the adequate amounts of the polyester diol PLGA, HDI, DMPA and Tin(II) 2-thylhexanoate in 5 ml of dimethyl sulfoxide. The reaction proceeded at 70 °C for 2 h under N_2 atmosphere and magnetic stirring. TEA was then added to neutralize −COOH groups of DMPA, and the reaction medium stirred for 30 min.

2.2.3. Synthesis of hydrogel based waterborne polyurethane-chitosan (HPUC)

Chitosan (0.01 g/mL) was solubilized in a 1 % acetic acid solution for 45 min at 40 °C in an ultrasonic bath. Before use, the Chitosan solution was filtered (45 μm filter) and transferred to an addition funnel. The Chitosan solution was added dropwise to the PU prepolymer solution under stirring at 70 °C. After homogenization, the final solution was cast in a poly(tetrafluor ethylene) Petri dish and kept in an air circulating oven at 60 °C for 24 h to allow the cross-linking reaction and solvent evaporation. The membranes thus formed were washed by immersion in deionized water for three days, changing the water every day. The membranes were finally washed with acetone in a refluxing apparatus for 4 h and then dried in a vacuum at room temperature.

2.3. Characterization of HPUC membranes

Infrared spectroscopy was performed on a Perkin-Elmer Spectrum 100 FT-IR (ATR) spectrometer. Solid- state ^{13}C NMR was performed on an Agilent DD2 500 MHz (11.7 T) NMR spectrometer. Thermogravimetric analyses were conducted on a Mettler-Toledo TGA/ SDTA851e –FL1600. The samples were heated from 30 °C to 900 °C at a 10 °C/min heating rate in an N_2 atmosphere (50 ml/min).

2.4. Solubility test and water uptake

The dry samples were cut into pieces weighing around 50 mg. For solubility tests, the samples were immersed in each solvent in a vial and shaken at room temperature. The water uptake of the samples after being immersed for different times was evaluated as:

$S = [(M_f - M_i/)M_i] * 100$, where:

M_i is the weight of the dry sample at time $t = 0$ s and M_f is the weight of the wet sample at immersion time t.

2.5. Degradation test

The dry samples were cut into pieces weighing around 50 mg and immersed in a vial with phosphate buffered saline, PBS (pH 7.4). The samples were placed in a shaking incubator at 37 °C. Buffer was changed weekly. All tests were performed in triplicate. After the periods of evaluation, the samples were removed from the buffer, gently dried with a filter paper and washed three times with deionized (DI) water and then dried in an oven for 24 h at 60 °C and immediately weighed.

The degradation ratio was determined according to the following equation:

$W_l = [(W_f - W_i/)W_i] * 100$; were:

W_l = weigth loss, W_i = Initial dry weight, W_f = dry weight after time degradation,

The results shown are the average of 3 replica.

2.6. In vitro and in vivo assay

This study was published and approved by the Health Sciences Commission of the School of Medicine of the Pontifícia Universidade Católica do Rio Grande do Sul - PUCRS under number 6236, and also by the Committee on Ethics in the Use of Animals - PUCRS, registered under number 15/00469. All procedures and techniques used during the animal experimentation are in accordance with the regulation proposed in the Brazilian Guidelines for the Care and Use of Animals for Scientific Purposes, by the National Council for the Control of Animal Experimentation (CONCEA) and the Ethics Committee for Use of Animals of PUCRS (CEUA).

2.6.1. Mononuclear bone marrow fraction isolation (BMMNCs)

After euthanasia the donor animals were dissected and bone marrow was aspirated from the long bones. The aspirated material was placed in falcon tubes containing RPMI medium and was transferred to another tube containing FicollPaque (Histopaque 1119, Sigma Aldrich) and centrifuged at 400 *g*. The mononuclear cell layer was collected and washed with Dulbecco's Phosphate Buffered Saline (DPBS). Viability was then determined using the trypan blue exclusion method. The same procedure was used for the tissue regeneration assay.

2.6.2. Cell culture

The cytotoxicity assay was performed with the adherent cell fraction. The cells were cultivated until confluence in a 75 cm^2 cell culture flask containing Dulbecco's modified Eagle's medium (DMEM), supplemented with 10 % of Fetal Bovine Serum (FBS), gentamicin (0.025 g/L and streptomycin/penicillin (0, 1 g/L) in humid atmosphere at 37 °C with 5 % of CO_2.

2.6.3. MTT assay

Cytotoxicity was evaluated according to ISO 10993-5, evaluating the mitochondrial function by tetrazolium salt reduction (MTT). The sample extracts were prepared in DMEM. After sterilization with ethanol, the HPUC membranes were washed by immersion in sterile Milli Q water three times and then once in DPBS and DMEM without FBS, immersed in DMEM medium for 24, 48 or 72 h and incubated with stirring in a humid atmosphere at 37 °C with 5 % of CO_2. DMEM medium was used as negative control and copper sulfate (0.1 g.mL^{-1}) in DMEM medium as positive control. All membranes were cut to a size of 3 cm^2 and were incubated in 5 ml DMEM to allow the extraction. The BMMNCs suspension was adjusted and seeded at a density of 0.5×10^4

cell per well onto 96-well culture plates and incubated for 24 h to allow cellular adhesion. The cells were then incubated for 24 h with DMEM and after that, the reading was performed. The absorbance values obtained were normalized by negative control with 100 % viable cells. All the tests were performed in triplicate.

2.6.4. Direct contact

The cells were seeded at a density of 5×10^4 cells per well onto a 24-well culture plate. The membrane was cut into a small circle (11-mm diameter) and placed in the middle of a well and incubated for 24 h, 48 h and 72 h in humid atmosphere at 37 °C with 5 % of CO_2. Cell viability was evaluated by the Live/Dead Cell Viability Assay on an Inverted Phase Contrast Fluorescence Microscope (Thermo Fischer Scientific) according to the manufacturer's instructions.

2.6.5. Animal model of diabetic ulcers

60 day-old adult female Wistar rats weighing between 200 and 300 g were given water and food ad libitum. Tail blood was collected at time 0 to evaluate the glycemic levels. All animals were fasted for 8 h prior to diabetes induction, which was by an intraperitoneal injection of Streptozocin (70 mg/kg). Seven days after the streptozotocin injection the blood glucose levels of the animals were measured by the Accu-Check Active kit (Roche Diagnostics GmbH). The animals with blood glucose levels above 250 mg/dl were considered diabetic. After glucose measurement, the animals were divided into two groups as described below. The animals submitted to the simulated ulcer procedure were given anesthesia of 80 % Ketamine and 20 % Chlorpromazine, followed by a dorsal incision of about 6 mm diameter with a scalpel to simulate an ulcer wound.

2.6.6. Experimental design and treatment of groups

In the *in vivo* evaluation for minimizing the use of animals, only HPUC1 membrane was selected because it is less fragile than HPUC2 and HPUC3 because its water sorption capacity is smaller while cytotoxicity results were similar in the three samples (see below). The 16 rats were divided into 2 groups: Group 1 (control) (n = 8): diabetic animals, with a wound, without treatment; Group 2 (n = 8): diabetic animals with HPUC and BMMNCs transplanted onto the wound site. After the formation of the wound, 1×10^6 cells of the mononuclear bone marrow fraction were transplanted into each animal in Group 2 by injection into the edge of the wound. After this procedure, the HPUC was positioned and sutured onto the wound. The animals were evaluated histologically in two different periods of time: 7 and 14 days after membrane implantation.

2.7. Histopathology of diabetic mice wounded skin tissues

Samples obtained from the histological analyses of the wound were removed 7 and 14 days after wound formation. To obtain the sample, the wounded area was removed from the animals backs after euthanasia in the CO_2 chamber. All the samples were fixed in neutral buffered formalin and embedded in paraffin wax. Each section was 4 μm thick and stained with hematoxylin-eosin (H&E). The analysis of the epithelial tissue and the depth of the epithelial cell-covered wound were considered. The analysis of connective tissue was considered for the study of the inflammatory process, measured by the type and quantity of inflammatory cells and presence / absence of fibrosis, using H&E staining. The analyses were performed by two blinded examiners, previously instructed by a pathologist and calibrated by the kappa coefficient-test.

2.8. Macroscopic wound closure analyses

The closure of the wounds was measured by comparing with ImageJ software the images recorded during the experiments. The formula used to measure the wound regeneration rate was as follows:
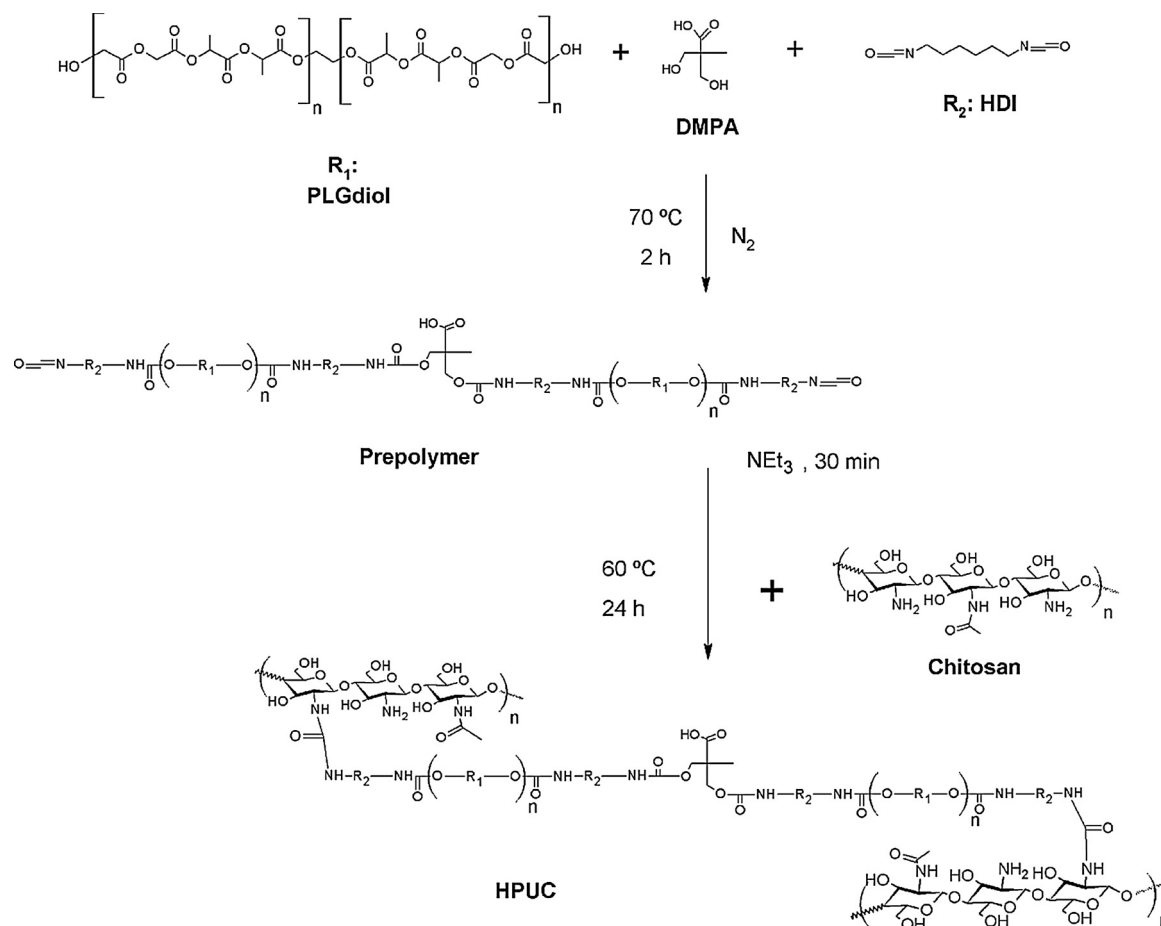
Fig. 1. Synthesis route of the HPUC membranes.

RWA = (DA)/(OWA)*100; were:

RWA: Residual wound área (%), DA: Detected Area, OWA: Original Wound Area.

2.9. Statistical analysis

Quantitative data was expressed as mean ± standard deviation. To compare the regeneration of the wound between the groups, an unpaired *t*-test was perfomed at each time to compare the difference in wound closures. Values with $p < 0.05$ were considered statistically significant. All the statistical analyses were performed with the statistical GraphPad Prism.

3. Results and discussion

3.1. Synthesis of hydrogel membranes

The chitosan waterborne polyurethane was obtained in two stages as shown in the reaction scheme in Fig. 1. The first (i) step consisted of the synthesis of the polyurethane prepolymer (PU prepolymer) with different weights of the soft segment poly (lactide-co-glicolide) diol, with HDI and DMPA as a chain extensor. In the second (ii) step, the HPUC was obtained by crosslinking reaction of the PU prepolymer with chitosan during membrane formation.

The synthesized membranes to be used as wound dressings were successfully obtained as shown in Fig. 1. However, the membrane (HPUC3) with the highest amount of prepolymer (75 %) became more brittle than the others (Fig. S1 in Supplementary material). This could have been due to the membrane presenting a phase separation, which may have contributed to the immiscibility of the components and making it brittle (T_g 15 °C, data not shown). This was not observed in the other two membranes.

3.2. Swelling

Chitosan was soluble in acetic acid 1 % while the prepolymers were soluble in DMSO, acetone and CHCl$_3$. The membranes were not soluble in the solvents used to solubilize the prepolymer or in acetic acid 1 %, proving the formation of crosslinked networks. Sample weight in immersion in liquid water stabilizes after 48 h (See Fig. S2 in Supplementary material). The water sorption capacity at 48 h for the different samples is larger than 1000 % measured on dry basis (Table 1). The network swelling capacity confirms that, contrary to what could be expected, the membrane with the highest hydrophobous component, HPUC3, had the highest water uptake. The water content measured at 48 h of immersion time thus fell from about 2000 to 1200 when the PLGA content was reduced from 75 % to 25 % (samples HPUC3 and HPUC1).The figure does not show a curve for pristine chitosan because it is water soluble, since the amine groups remain protonated after dissolution in the acidic medium. Hydrogel equilibrium water content is described by the Flory Rhener Equation (Flory & Rehner, 1943), which shows that swelling increases with a favorable water-polymer segment interaction parameter and with the higher average molecular weight between crosslinks in the network, i.e. with a reduced crosslinking density. The higher PLGA/CHS ratio should yield a less favorable average interaction parameter between PU soft segments and water. The fact that swelling capacity nevertheless increases could be due to less efficient crosslinking with the presence of a significant number of unreacted carboxyl end groups in PU prepolymer.
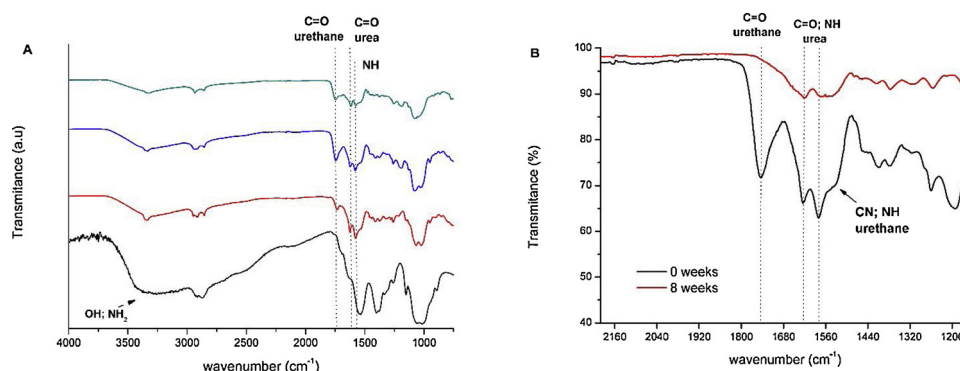
Fig. 2. FTIR spectrum of membranes. (A) Membranes before the degradation test. Arrows and lines indicate the main groups related to crosslinking between the prepolymer PU and CHS (in black: CHS, red: HPUC1, blue: HPUC2 and green: HPUC3). (B) Membrane HPUC2 after 8 weeks immersion in PBS 1x buffer.

3.3. FT-IR of chitosan polyurethane

The spectra of original chitosan and polyurethane based on chitosan with different soft segment contents are shown in Fig. 2A.

The chitosan spectrum shows the typical large peaks in the 3340 cm-1 region relative to the stretching of the OH and NH2 groups, 2872–2920 cm-1 to CH2 stretch, 1151 cm-1 for C−O−C of the chitosan ring. The appearance of the peaks relative to urea and urethane bonds can be observed in the case of polyurethane prepolymer and the networks. The membrane formed has two hard segments due to the urea and urethane bonds formed between the diisocyanate groups and NH$_2$ and OH chitosan groups and PLGA/DMPA, respectively (Subramani, Park, Lee, & Kim, 2003). These urethane bond peaks appear in the 1730–1746 cm-1 region (C=O stretch), 1027–1074 cm-1 (C−O stretch) and urea bonds at 1616–1625 cm-1 (C=O stretch), 1589 cm-1 (NH bending) and 1254–1260 cm-1 (C−N stretch). As found by other authors, the urea bond formation (−NHCONH−) occurs because the preferential reactivity of NCO groups with NH$_2$ groups is much more reactive than the OH groups (Chen et al., 2012; Pérez-Limiñana, Arán-Aís, Torró-Palau, Orgilés-Barceló, & Martín-Martínez, 2005; Velazquez-Morales, Le Nest, & Gandini, 1998).

In the supplementary data, Fig. S3, the FTIR spectra of the synthesized PLGAdiol and the PU prepolymer are shown. Although is observed an overlapping in the urethane and urea absorption region the peaks around 1600–1750 cm-1 are distinguishable. The presence of the absorption band at 1625 cm-1, which is ascribed to hydrogen-bonded urea groups (Marchant, Zhao, Anderson, & Hiltner, 1987; Zhang, Ren, He, Zhu, & Zhu, 2007) and is absent in the prepolymer is slightly different in the networks with varying composition, showing that sample composition affects the reaction mechanism.

3.4. Solid state ^{13}C-NRM

Fig. 3 shows the solid state NRM spectra of chitosan and HPUC membranes with 25 % (HPUC1), 50 % (HPUC2) and 75 % (HPUC3) soft segment. In chitosan the peaks in Fig. 3 are those of C1 (δ104.8), C4 (δ81.5), C5 and C3 (δ75.1), C6 and C2 (δ57.2), and CH3 (δ22.6), in agreement with other studies (de Moura, Aouada, & Mattoso, 2008; Heux, Brugnerotto, Desbrières, Versali, & Rinaudo, 2000). For HPUC membranes we observed novel peaks, which have been reported as the chitosan-PU crosslinking for HPUC1 peaks: δ174.82, δ159.27, δ99.49, δ73.24, δ60.60, δ41.65, δ29.50, δ17.34; for HPUC2: δ176.77, δ159.76, δ101.92, δ73.24, δ61.09, δ41.65, δ29.98, δ16.86 and HPUC3: δ174.34, δ159.27, δ102.40, δ74.40, δ60.60, δ42.13, δ30.64, δ23.13. The carbonyl (CO) shifts are far from the field (155 − 210 ppm) and generally weak due to slow relaxation. For urea and urethanes the shifts are 170–180 and 150–160, respectively. The peak of ^{13}C spectra in the urea group occurs at a higher magnetic field than those in the urethane group (Zhang, Cheng, & Hu, 2003). The displacement, found in HPUCs
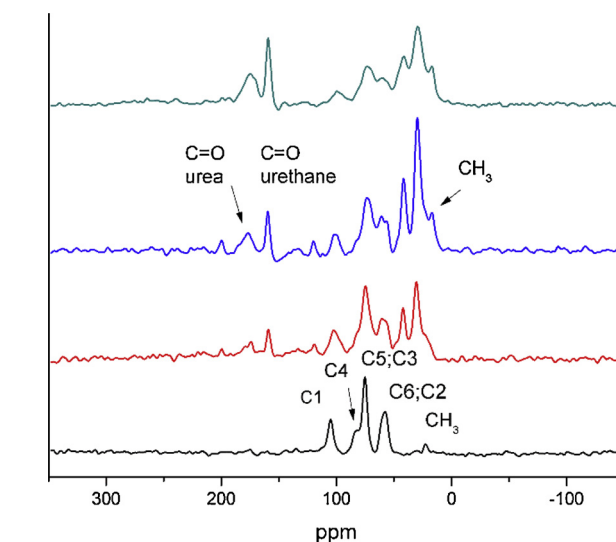

Fig. 3. Solid state ^{13}C-NRM spectrum of membranes. Arrows indicate the main shifts related to crosslinking between the prepolymer PU and CHS (in black: CHS, red: HPUC1, blue: HPUC2 and green: HPUC3).

around δ174, is related to urea bounds between –NH$_2$ groups of chitosan and −NCO groups of PU prepolymer, while δ159 is related to both urethane bonds −NHCOO− of polyester and DMPA in the soft and hard segments, respectively (Barikani et al., 2010; Leventis et al., 2010).

3.5. Thermogramymetric analysis

Fig. 4B show the derivative weight loss (DTG) curves of chitosan and HPUC membranes. In the chitosan and HPUC TG curve we observed the first thermal event in the 40 − 140 °C range, which indicates a weight loss of less than 6 % attributed to the evaporation of residual water from the polymer (de Britto & Campana-Filho, 2007). The second thermal event, after 140 °C, is due to the overlapping of the degradation of chitosan and PLGA chains. Thermal degradation of the chitosan used in this study takes place in the 187 − 372 °C range (with a maximum in the DTG plot at 268 °C) and is attributed to the thermal decomposition of chitosan chains (Abused et al., 2014; Neto et al., 2005; Zawadzki & Kaczmarek, 2010). For HPUCs, thermal decomposition in the TG curve occurs in a broader temperature range between 142 and 502 °C. The overlap of the different phenomena can best be seen in the DTG curve (Fig. 4B).

The peak appearing at the lower temperature is attributed to the degradation and weight loss of the hard and soft segments of the urethane groups (the intensity of this peak increases with increasing PLGA content, as expected). This peak appears at temperatures lower than
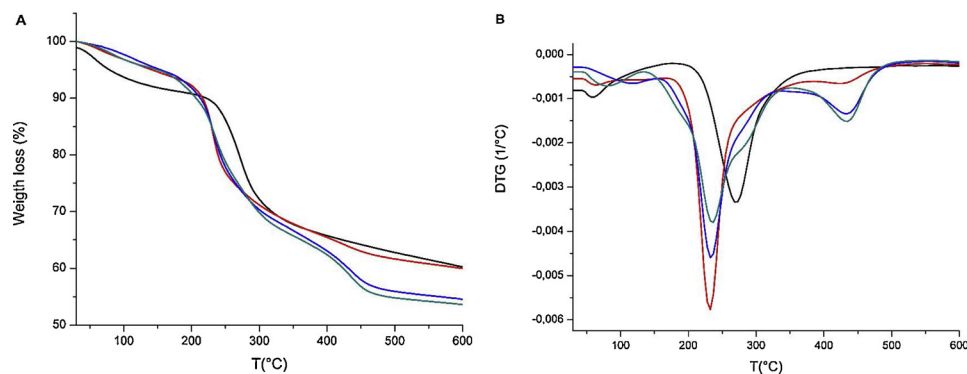
Fig. 4. Graphs of the relative weight loss curves (A) and derived weight loss (B) of chitosan membranes and HPUCs (in black: CHS, red: HPUC1, blue: HPUC2 and green: HPUC3).

Table 2
Maximum degradation temperature of CHS and HPUCs.

Sample	Temperature range ºC	Second Stage T_{max} (ºC)	Third Stage T_{max} (ºC)	Weight loss %
CHS	187–372	268		30
HPUC1	171–476	232.5	426	36
HPUC2	151–507	232.5	435	40
HPUC3	142–507	237	435	41

that of pure chitosan degradation (the maximum in DTG curve appears at ∼235 °C). On the high temperature side of this peak, in the chitosan degradation temperature range a shoulder can be seen indicating the decomposition of chitosan chains in the network. The highest temperature peak in the HPUCs is relative to the weight loss of the hard segment of the urea bond, since the energy of the urea bond is larger than that of the urethane bond, the degradation peak in urea appears at higher temperatures (García-Pacios, Costa, Colera, & Martín-Martínez, 2011). Table 2 gives the chitosan and HPUC thermal data. HPUC membranes had a lower onset temperature, HPUC1 > HPUC2 > HPUC3, with PLGA incorporated in the chitosan structure, which could be associated with changes in the intermolecular interactions between polysaccharide chains resulting in reduced polymer thermal stability.

3.6. Degradation in PBS medium

Fig. 5 shows the degradation curves in an aqueous solution (PBS 1x pH 7.4) for up to eight weeks. There is a significant mass loss at the end of the eight weeks in the HPUC2 and HPUC3 samples, 87.0 % and 90.5
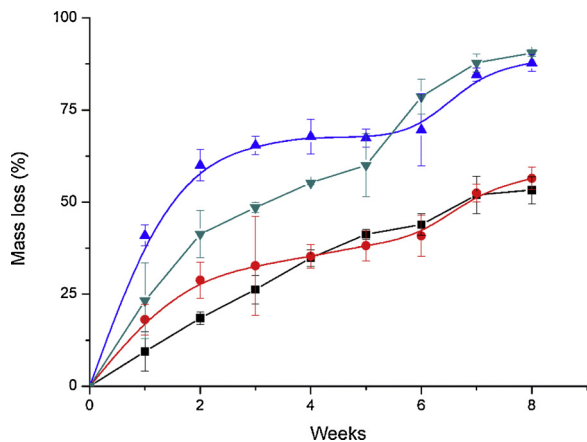

Fig. 5. CHS and HPUC mass loss curves after up to eight weeks: ■ CHS, ● HPUC1, ▼HPUC2 and ▲HPUC3. All values are expressed as mean ± standard deviation (n = 3).

% respectively, compared to 56.4 % for HPUC1 and 53.2 % for CHS. The findings show that membrane weight loss has two different mechanisms. Since the membranes were not neutralized at the end of the synthesis, one could expect that the chitosan chain amine groups would remain protonated and that the chitosan would be slowly dissolved in the aqueous solution. Thus, the pure chitosan film presents a continuous weight loss of up to 53.2 %, which cannot be explained by hydrolysis. This delivery of chitosan chains by dissolution in the aqueous medium is prevented in the HPUC hydrogels by the polymer network structure. Nevertheless, HPUC2 and HPUC3 membranes can degrade by nearly 100 % in eight weeks. Since cleavage of chitosan chains by hydrolysis does not take place in the degradation times of our experiments, we hypothesize that the cleavage of the PLGA chains and urea linkages liberates chitosan chains that are susceptible to being dissolved in the medium, since they are protonated, contributing to the weight loss (See the schema in Fig. S4 of Supplementary material).

FTIR analysis support this assumption. After eight weeks of degradation of the HPUC membranes (Fig. 2B) it is clear the disappearance of the peaks characteristic of the PU regions between 1500-1150 cm-1, and the strong band at approximately 1745 cm-1 corresponding to a C=O bond of ester groups showing the degradation of the PLGA segment. In addition, the original position of the amide peak at 1579 cm-1 (C−N and N−H) moves to 1575 cm-1 (Fig. 2B). It is also possible to visualize the displacement of the 1625 cm-1 peak for 1619 cm-1 corresponding to the carbonyl bond in the urea groups (C=O amide I) indicating degradation of the rigid segment ((Marcos-Fernández, Abraham, Valentín, & Román, 2006; Pretsch, Jakob, & Müller, 2009), the same can be seen in the 1530 cm-1 region referring to PU urethane group bound to the CHS chains.

The high swelling capacity of the HPUC network, even for the largest PLGA content, contributes to the hydrolysis process. PLGA chains are exposed to water molecules in the swollen sample and thus the hydrolysis of the ester groups is faster than in bulk PLGA which is highly hydrophobous.

Thus, we propose that the fast, and nearly complete degradation of the HPUC hydrogels is due to the combination of the loose of the degradation fragments of PLGA chains together with the delivery of CHS chains detached from the network structure.

3.7. In vitro cytotoxicity analysis of HPUC membranes

To select the best membrane to continue the *in vivo* assay we evaluated cellular viability by mitochondrial metabolic activity. For the indirect cytotoxicity analysis, the adherent BMMNCs were cultured with membrane extracts obtained after immersion of the membranes for periods of 24, 48 and 72 h. The viability of the cells cultured in direct contact with HPUC membranes in the same time periods was assessed with a live/dead test with fluorescence microscopic evaluation. In all the exposure periods in the indirect contact experiment the
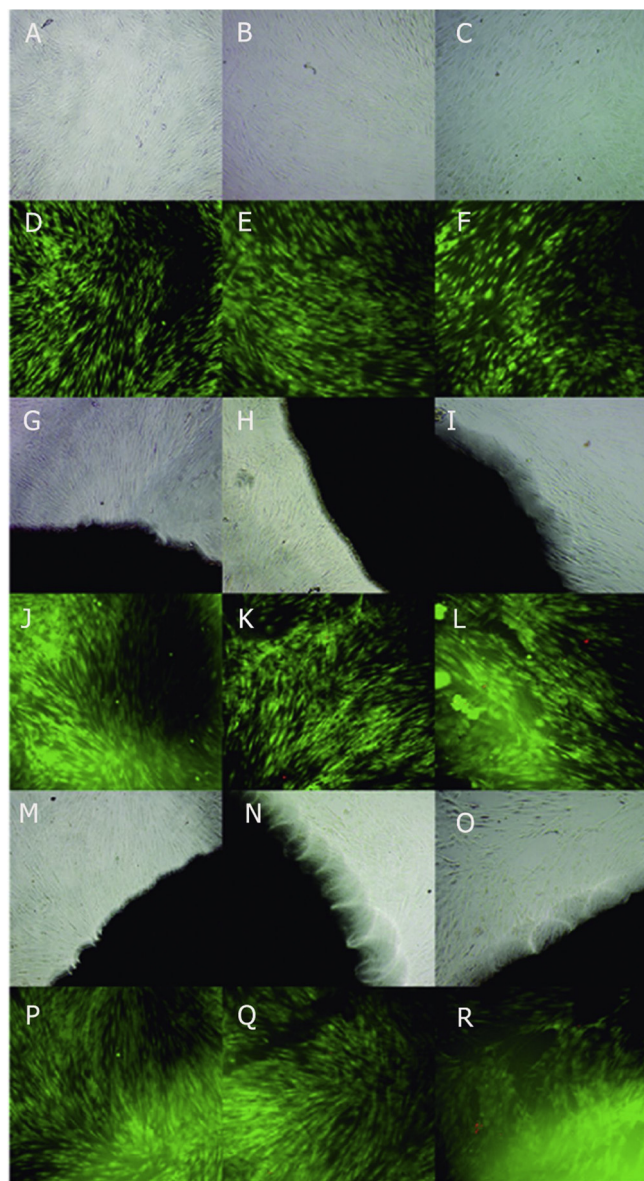
Fig. 6. Representative fluorescent image of MSCs: (A–F) Control, (G–L), HPUC2, (M–R), HPUC1. Live cells were stained with calcein AM (green) using a FITC filter and dead cells were stained with Ethidium homodimer (red) and captured by an PI filter. All images were acquired after 24, 48 and 72 h. Magnification $100\times$.

viability was of all the membranes above 80 % of the negative control (Fig. S5 in Supplementary material)

Considering the results obtained for HPUC3 degradation time and brittleness in the swelling experiments, we opted for HPUC1 and HPUC2 membranes to continue the evaluation. The HPUC1 and HPUC2 networks were analyzed in direct contact using the live/dead fluorescence assay, which provides information on physical cell properties (cellular membrane integrity) and biochemical intracellular esterase activity (Masson-Meyers, Bumah, & Enwemeka, 2016). No cytotoxicity effect was detected (see images in Fig. 6), indicating that the cells produced esterase (green fluorescence), which is an indicator of viable cells, while the red fluorescence that indicates cell death is rarely observed. The images show the cells well spread out on the culture plate, while the morphology and cell numbers are quite similar to those of the controls.

3.8. HPUC plus BMMNCs accelerated wound repair in diabetic rats

Considering the high costs of treating patients with ulcers in the lower limbs, and the high morbidity and mortality rate caused by this type of wound, the research for new treatments is necessary. Diabetic patients affected by ulcers in the lower limbs go through a prolonged inflammatory phase during tissue regeneration, with persistence of a pro-inflammatory profile, moving from an acute to a chronic state. This prolonged inflammation is directly related to the precarious healing of these wounds, leading these individuals to recurrent infections, and when not properly treated at an early stage, can lead to amputation. Our study aimed to identify whether the use of a biological dressing associated with mononuclear bone marrow fraction cells from rats would be able to improve the regenerative response in ulcerous wounds in diabetic rats.

From an intraperitoneal use of streptozotocin, it was possible to establish an animal model of diabetes. After the model was established, we were able to create a wound on the animals' backs to simulate an ulcer wound, simulating the ulcer shown in lower limbs from diabetic individuals. From the results, it was observed that the group of animals treated with the HPUC combined with the injection of BMMNCs in the interphase between the tissue and the HPUC membrane (Group 2) showed significantly better results in terms of healing in the first 7 days after the formation of the wound compared to the control group (Fig. 7). During the first few days, we observed that the animals that had the HPUC plus BMMNCs on the wound had a cleaner and drier wound, when compared macroscopically with the animals that did not receive the treatment. This suggests that the membrane achieved hemostasis of the wound, supporting the formation of the fibrin matrix and cell infiltration (Eming, Martin, & Tomic-canic, 2014; Oberyszyn, 2008).

In addition, the animals treated with the BMMNCs plus the biomaterial showed a significantly better regeneration rate than those from the control group after 14 days, with a significant reduction in wound size.

The use of bone marrow-derived mesenchymal cells enhances tissue regeneration, significantly reducing the wound size in rat diabetes ulcer models using streptozotocin. In addition, complete wound healing time was also significantly lower in the mesenchymal cell treated group (Kuo et al., 2011). The combination BMMNCs and HPUC provided wound healing in just 14 days (wound closure > 90 %). Although previous studies in the literature with different biomaterials showed a significant improvement of wound healing, they required longer times and a more intense inflammatory process (Ahmed et al., 2018; Sayed et al., 2016). The macroscopic analysis of wounds treated with these membranes revealed a considerably smaller wound bed than those in the control group.
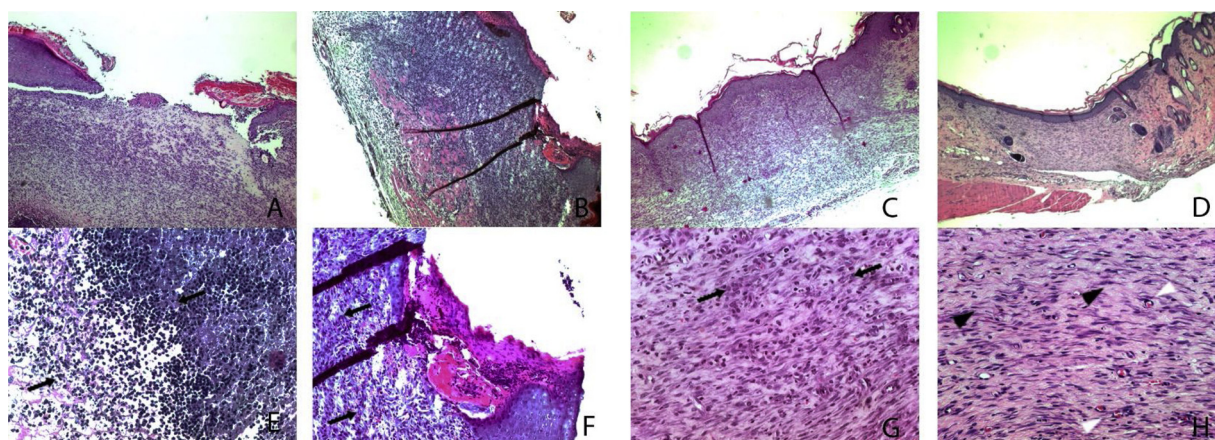
3.9. Histological wound healing by H&E staining

To evaluate the role of BMMNCs in the remodeling and speed of tissue regeneration when transplanted with a HPUC membrane, we collected the samples from the wound region in the diabetic rats for histological analysis on days 7 and 14. On day 7 it was observed a noticeable difference on wound closure from the treated group (Fig. 8) compared to the non-treated group.

Unlike Group 2 (HPUC + BMMNCs), Inflammatory cell infiltrate was observed in the control group and there were no signs of epithelial regeneration. In Group 2, moderate inflammatory infiltrate was visible, together with wound closure with epithelization. On day 14 remodeling of the wound was clearly seen in Group 2 with organized connective tissue and neovascularization, indicating successful healing. This was not found in the control group.

Initial inflammation at the beginning of healing is critical for the regeneration period, which dictates the second phase of wound regeneration, with reduced inflammation remodeling and culminating in
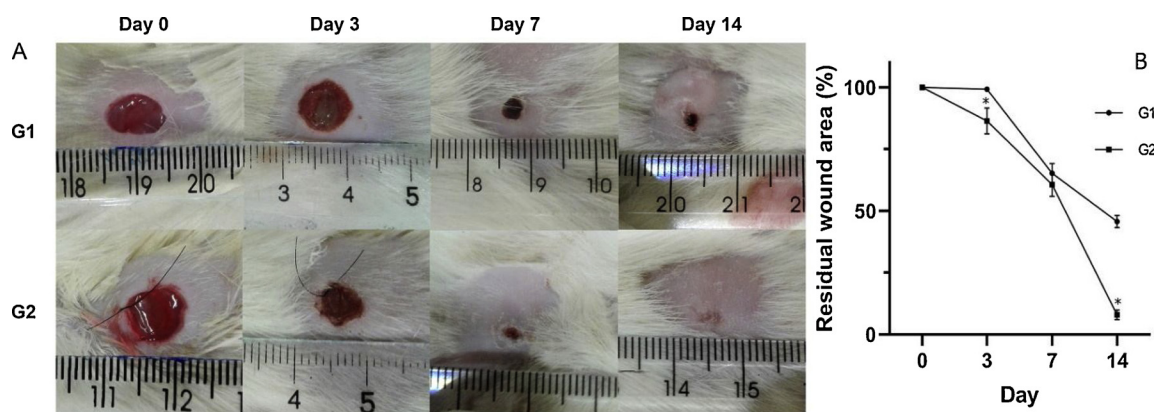
Fig. 7. Representative image in the effects of HPUC1 and BMMNCs on wound healing in diabetic ulcer model. (A) Macroscopic observations in wound areas in the control (G1) and wound healing contraction induced by HPUC1 plus BMMNCs (G2). (B) Residual wound area. The results are expressed as mean ± standard deviation (n = 6). (*) indicates significant difference, p < 0.05.

Fig. 8. Representative histologic analysis of the wound region. Tissue samples were collected on day 7 (**A, E, C, G**) and 14 (**B, F, D, H**). H&E staining showed severe nflammation in the control group (**A, B, E, F**) and wound healing and re-epithelialization (**C, D, G, H**) in the HPUC1 plus BMMNC group. Black arrows indicate inflammatory cell infiltrate, black arrowhead fibroblasts and white arrowhead indicate blood vessels. Magnification 4x in A, E, C, D, and 20x in B, F, G, H.

wound closure (Koehler, Brandl, & Goepferich, 2018). All these processes involve several cell types. The mesenchymal cells in the BMMNC fraction of bone marrow aspirates may have a positive effect on the anti-inflammatory process for their differentiation and paracrine effects (Chen, Tredget, Wu, Wu, & Wu, 2008; Park, Ahn, Sung, Ahn, & Chang, 2018). Another important point was the large HPUC membrane water absorption capacity (shown in swelling tests). Better dressing water uptake could lead to different forms of exudate retention, which may cause changes in cytokine levels and growth factors on the wound surface and faster cicatrization (Yamane et al., 2015).

4. Conclusions

This paper describes a study of synthesized chitosan/PLGA networks, which were found to present continuous degradation in aqueous solution. The hydrolytic degradation of polyurethane blocks liberated chitosan chains that dissolved in the aqueous solution. We confirmed that this biomaterial has low cytotoxicity and supports cell proliferation. The synthesis was based on unmodified chitosan and new crosslinkers consisting of a low molecular weight polyester polyurethane with NCO terminations, enabling crosslinking with free amine of chitosan. The use of BMMNCs helped to close the wounds, reduce inflammation and improve neovascularization around the wound. The results show that the synthesized hydrogel plus BMMNCs is suitable for use as a dressing for diabetic wounds and has a potential use in tissue engineering.

Appendix A. Supplementary data

Supplementary material related to this article can be found, in the online version, at doi:https://doi.org/10.1016/j.carbpol.2019.115734.

References

Abused, W., Doe, J., Ad, G. R., Lo, B. I. O., Man, G.-H. U., Oach, A., ... Ward, G. (2014). From the SAGE social science collections. All rights reserved. *Journal of Composite*

Materials, 16(4), 928–940. https://doi.org/0803973233.

Ahmed, R., Tariq, M., Ali, I., Asghar, R., Noorunnisa Khanam, P., Augustine, R., ... Hasan, A. (2018). Novel electrospun chitosan/polyvinyl alcohol/zinc oxide nanofibrous mats with antibacterial and antioxidant properties for diabetic wound healing. *International Journal of Biological Macromolecules, 120*, 385–393. https://doi.org/10.1016/j.ijbiomac.2018.08.057.

Andrade, F., Goycoolea, F., Chiappetta, D., das Neves, J., Sosnik, A., & Sarmento, B. (2011). Chitosan-grafted copolymers and chitosan-ligand conjugates as matrices for pulmonary drug delivery. *International Journal of Carbohydrate Chemistry, 2011*, 1–14. https://doi.org/10.1155/2011/865704.

Baltzis, D., Eleftheriadou, I., & Veves, A. (2014). Pathogenesis and treatment of impaired wound healing in diabetes mellitus: New insights. *Advances in Therapy, 31*(8), 817–836. https://doi.org/10.1007/s12325-014-0140-x.

Barikani, M., Honarkar, H., & Barikani, M. (2010). Synthesis and characterization of chitosan-based polyurethane elastomer dispersions. *Monatshefte Fur Chemie, 141*(6), 653–659. https://doi.org/10.1007/s00706-010-0309-1.

Boulton, A. J. M. (2013). The pathway to foot ulceration in diabetes. *The Medical Clinics of North America, 97*(5), 775–790. https://doi.org/10.1016/j.mcna.2013.03.007.

Casettari, L., Vllasaliu, D., Castagnino, E., Stolnik, S., Howdle, S., & Illum, L. (2012). PEGylated chitosan derivatives: Synthesis, characterizations and pharmaceutical applications. *Progress in Polymer Science, 37*(5), 659–685. https://doi.org/10.1016/j.progpolymsci.2011.10.001.

Chen, L., Tredget, E. E., Wu, P. Y. G., Wu, Y., & Wu, Y. (2008). Paracrine factors of mesenchymal stem cells recruit macrophages and endothelial lineage cells and enhance wound healing. *PLoS One, 3*(4), https://doi.org/10.1371/journal.pone.0001886.

Chen, S. H., Tsao, C. T., Chang, C. H., Wu, Y. M., Liu, Z. W., Lin, C. P., ... Hsieh, K. H. (2012). Synthesis and characterization of thermal-responsive chitin-based polyurethane copolymer as a smart material. *Carbohydrate Polymers, 88*(4), 1483–1487. https://doi.org/10.1016/j.carbpol.2012.01.055.

Tsao, C. T., Chang, C. H., Li, Y. D., Ming Fung, W., Lin, C. P., Han, J. L., ... Hsieh, K. H. (2011). Development of chitosan/ dicarboxylic acid hydrogels as wound dressing materials. *Journal of Bioactive and Compatible Polymers, 26*(5), 519–536. https://doi.org/10.1177/0883911511422627.

de Britto, D., & Campana-Filho, S. P. (2007). Kinetics of the thermal degradation of chitosan. *Thermochimica Acta, 465*(1–2), 73–82. https://doi.org/10.1016/j.tca.2007.09.008.

de Moura, M. R., Aouada, F., & Mattoso, L. H. C. (2008). Preparation of chitosan nanoparticles using methacrylic acid. *Journal of Colloid and Interface Science, 321*(2), 477–483. https://doi.org/10.1016/j.jcis.2008.02.006.

Dinh, T., Tecilazich, F., Kafanas, A., Doupis, J., Gnardellis, C., Leal, E., ... Veves, A. (2012). Mechanisms involved in the development and healing of diabetic foot ulceration. *Diabetes, 61*(11), 2937–2947. https://doi.org/10.2337/db12-0227.

Eming, S. A., Martin, P., & Tomic-canic, M. (2014). STATE OF THE ART REVIEW Wound repair and regeneration: Mechanisms, signaling, and translation. *Science Translational Medicine, 6*(265), 265sr6. https://doi.org/10.1126/scitranslmed.3009337.

Escobar Ivirico, J. L., Salmerón-Sánchez, M., Gómez Ribelles, J. L., & Monleón Pradas, M. (2009). Poly(L-lactide) networks with tailored water sorption. *Colloid and Polymer Science, 287*(6), 671–681. https://doi.org/10.1007/s00396-009-2026-z.

Flory, P. J., & Rehner, J. (1943). Statistical mechanics of cross-linked polymer networks II. Swelling. *The Journal of Chemical Physics, 11*(11), 521–526. https://doi.org/10.1063/1.1723792.

Gámiz-González, M. A., Vidaurre, A., & Gómez Ribelles, J. L. (2017). Biodegradable chitosan-poly(ε-caprolactone) dialdehyde copolymer networks for soft tissue engineering. *Polymer Degradation and Stability, 138*, 47–54. https://doi.org/10.1016/j.polymdegradstab.2017.02.005.

García-Pacios, V., Costa, V., Colera, M., & Martín-Martínez, J. M. (2011). Waterborne polyurethane dispersions obtained with polycarbonate of hexanediol intended for use as coatings. *Progress in Organic Coatings, 71*, 136–146. https://doi.org/10.1016/j.porgcoat.2011.01.006.

Cruz, G., Dunia, M., Gomez Ribelles, J. L., & Salmerón Sánchez, M. (2008). Blending polysaccharides with biodegradable polymers. I. Properties of chitosan/polycaprolactone blends. *Journal of Biomedical Materials Research - Part B Applied Biomaterials, 85*(2), 303–313. https://doi.org/10.1002/jbm.b.30947.

Cruz, G., Mercedes, D., Salmerón-Sánchez, M., & Gómez-Ribelles, J. L. (2012). Stirred flow bioreactor modulates chondrocyte growth and extracellular matrix biosynthesis in chitosan scaffolds. *Journal of Biomedical Materials Research - Part A, 100 A*(9), 2330–2341. https://doi.org/10.1002/jbm.a.34174.

Heux, L., Brugnerotto, J., Desbrières, J., Versali, M. F., & Rinaudo, M. (2000). Solid state NMR for determination of degree of acetylation of chitin and chitosan. *Biomacromolecules, 1*(4), 746–751.

Hilfiker, A., Kasper, C., Hass, R., & Haverich, A. (2011). Mesenchymal stem cells and progenitor cells in connective tissue engineering and regenerative medicine: Is there a future for transplantation? *Langenbeck's Archives of Surgery, 396*(4), 489–497. https://doi.org/10.1007/s00423-011-0762-2.

Hilmi, A. B. M., Halim, A. S., Hassan, A., Lim, C. K., Noorsal, K., & Zainol, I. (2013). In vitro characterization of a chitosan skin regenerating template as a scaffold for cells cultivation. *SpringerPlus, 2*(2002), 79. https://doi.org/10.1186/2193-1801-2-79.

Hu, Y., Liu, Y., Qi, X., Liu, P., Fan, Z., & Li, S. (2012). Novel bioresorbable hydrogels prepared from chitosan-graft-polylactide copolymers. *Polymer International, 61*, 74–81. https://doi.org/10.1002/pi.3150.

Jiang, T., Nukavarapu, S. P., Deng, M., Jabbarzadeh, E., Kofron, M. D., Doty, S. B., ... Laurencin, C. T. (2010). Chitosan-poly(lactide-co-glycolide) microsphere-based scaffolds for bone tissue engineering: In vitro degradation and in vivo bone regeneration studies. *Acta Biomaterialia, 6*(9), 3457–3470. https://doi.org/10.1016/j.actbio.2010.03.023.

Jiang, X., Li, J., Ding, M., Tan, H., Ling, Q., Zhong, Y., ... Fu, Q. (2007). Synthesis and degradation of nontoxic biodegradable waterborne polyurethanes elastomer with poly(??-caprolactone) and poly(ethylene glycol) as soft segment. *European Polymer Journal, 43*(5), 1838–1846. https://doi.org/10.1016/j.eurpolymj.2007.02.029.

Jovanovic, D., Engels, G. E., Plantinga, J., Bruinsma, M., Van Oeveren, W., Schouten, a. J., ... Harmsen, M. C. (2010). Novel polyurethanes with interconnected porous structure induce in vivo tissue remodeling and accompanied vascularization. *Journal of Biomedical Materials Research - Part A, 95*(1), 198–208. https://doi.org/10.1002/jbm.a.32817.

Koehler, J., Brandl, F. P., & Goepferich, A. M. (2018). Hydrogel wound dressings for bioactive treatment of acute and chronic wounds. *European Polymer Journal, 100*(December 2017), 1–11. https://doi.org/10.1016/j.eurpolymj.2017.12.046.

Kuo, Y. R., Wang, C. T., Cheng, J. T., Wang, F. S., Chiang, Y. C., & Wang, C. J. (2011). Bone marrow-derived mesenchymal stem cells enhanced diabetic wound healing through recruitment of tissue regeneration in a rat model of streptozotocin-induced diabetes. *Plastic and Reconstructive Surgery, 128*(4), 872–880. https://doi.org/10.1097/PRS.0b013e3182174329.

Leventis, N., Sotiriou-Leventis, C., Chandrasekaran, N., Mulik, S., Larimore, Z. J., Lu, H., ... Mang, J. T. (2010). Multifunctional polyurea aerogels from isocyanates and water. A structure-property case study. *Chemistry of Materials, 22*(24), 6692–6710. https://doi.org/10.1021/cm102891d.

Marchant, R. E., Zhao, Q., Anderson, J. M., & Hiltner, A. (1987). Degradation of a poly (ether urethane urea) elastomer: Infra-red and XPS studies. *Polymer, 28*(12), 2032–2039. https://doi.org/10.1016/0032-3861(87)90037-1.

Marcos-Fernández, A., Abraham, G. A., Valentín, J. L., & Román, J. S. (2006). Synthesis and characterization of biodegradable non-toxic poly(ester-urethane-urea)s based on poly(ε-caprolactone) and amino acid derivatives. *Polymer, 47*(3), 785–798. https://doi.org/10.1016/j.polymer.2005.12.007.

Masson-Meyers, D. S., Bumah, V. V., & Enwemeka, C. S. (2016). A comparison of four methods for determining viability in human dermal fibroblasts irradiated with blue light. *Journal of Pharmacological and Toxicological Methods, 79*, 15–22. https://doi.org/10.1016/j.vascn.2016.01.001.

Merchant, Z., Taylor, K. M. G., Stapleton, P., Razak, S., Kunda, N., Alfagih, I., ... Somavarapu, S. (2014). Engineering hydrophobically modified chitosan for enhancing the dispersion of respirable microparticles of levofloxacin. *European Journal of Pharmaceutics and Biopharmaceutics, 88*(3), 816–829. https://doi.org/10.1016/j.ejpb.2014.09.005.

Moise, M., Sunel, V., Holban, M., Popa, M., Desbrieres, J., Peptu, C., ... Lionte, C. (2012). Double crosslinked chitosan and gelatin submicronic capsules entrapping aminoacid derivatives with potential antitumoral activity. *Journal of Materials Science, 47*(23), 8223–8233. https://doi.org/10.1007/s10853-012-6719-1.

Neto, C. G. T., Giacometti, J., Job, a. E., Ferreira, F. C., Fonseca, J. L. C., & Pereira, M. R. (2005). Thermal analysis of chitosan based networks. *Carbohydrate Polymers, 62*(2), 97–103. https://doi.org/10.1016/j.carbpol.2005.02.022.

Oberyszyn, T. M. (2008). *Department of pathology.* Columbus, OH: The Ohio State University2993–2999 43210 (8).

Ouyang, Q. Q., Hu, Z., Lin, Z. P., Quan, W. Y., Deng, Y. F., Li, S. D., ... Chen, Y. (2018). Chitosan hydrogel in combination with marine peptides from tilapia for burns healing. *International Journal of Biological Macromolecules, 112*, 1191–1198. https://doi.org/10.1016/j.ijbiomac.2018.01.217.

Page, J. M., Prieto, E. M., Dumas, J. E., Zienkiewicz, K. J., Wenke, J. C., Brown-Baer, P., ... Guelcher, S. (2012). Biocompatibility and chemical reaction kinetics of injectable, settable polyurethane/allograft bone biocomposites. *Acta Biomaterialia, 8*(12), 4405–4416. https://doi.org/10.1016/j.actbio.2012.07.037.

Park, W. S., Ahn, S. Y., Sung, S. I., Ahn, J. Y., & Chang, Y. S. (2018). Strategies to enhance paracrine potency of transplanted mesenchymal stem cells in intractable neonatal disorders. *Pediatric Research, 83*(1–2), 214–222. https://doi.org/10.1038/pr.2017.249.

Pérez-Limiñana, M. A., Arán-Aís, F., Torró-Palau, A. M., Orgilés-Barceló, a. C., & Martín-Martínez, J. M. (2005). Characterization of waterborne polyurethane adhesives containing different amounts of ionic groups. *International Journal of Adhesion & Adhesives, 25*(6), 507–517. https://doi.org/10.1016/j.ijadhadh.2005.02.002.

Pretsch, T., Jakob, I., & Müller, W. (2009). Hydrolytic degradation and functional stability of a segmented shape memory poly(ester urethane). *Polymer Degradation and Stability, 94*(1), 61–73. https://doi.org/10.1016/j.polymdegradstab.2008.10.012.

Rowlands, a. S., Lim, S., Martin, D., & Cooper-White, J. J. (2007). Polyurethane/poly (lactic-co-glycolic) acid composite scaffolds fabricated by thermally induced phase separation. *Biomaterials, 28*(12), 2109–2121. https://doi.org/10.1016/j.biomaterials.2006.12.032.

Sayed, O. N., Abdel-Rahman, R. M., Pavliňák, D., Abdel-Mohsen, A. M., Jancar, J., Burgert, L., ... Fohlerova, Z. (2016). Wound dressing based on chitosan/hyaluronan/nonwoven fabrics: Preparation, characterization and medical applications. *International Journal of Biological Macromolecules, 89*, 725–736. https://doi.org/10.1016/j.ijbiomac.2016.04.087.

Subramani, S., Park, Y., Lee, Y., & Kim, J. (2003). New development of polyurethane dispersion derived from blocked aromatic diisocyanate. *Progress in Organic Coatings, 48*, 71–79. https://doi.org/10.1016/S0300-9440(03)00118-8.

Tao, Z., Shi, A., & Zhao, J. (2015). Epidemiological perspectives of diabetes. *Cell Biochemistry and Biophysics, 73*(1), 181–185. https://doi.org/10.1007/s12013-015-0598-4.

Ünlü, C. H., Pollet, E., & Avérous, L. (2018). Original macromolecular architectures based on poly(ε-caprolactone) and poly(ε-thiocaprolactone) grafted onto chitosan backbone. *International Journal of Molecular Sciences, 19*, 3799. https://doi.org/10.3390/ijms19123799.

Velazquez-Morales, P., Le Nest, J.-F., & Gandini, A. (1998). Polymer electrolytes derived from chitosan/polyether networks. *Electrochimica Acta, 43*(10–11), 1275–1279.

https://doi.org/10.1016/S0013-4686(97)10030-5.

Wang, W., Ping, P., Chen, X., & Jing, X. (2006). Polylactide-based polyurethane and its shape-memory behavior. *European Polymer Journal, 42*(6), 1240–1249. https://doi.org/10.1016/j.eurpolymj.2005.11.029.

Yamane, T., Nakagami, G., Yoshino, S., Shimura, M., Kitamura, A., Kobayashi-Hattori, K., ... Sanada, H. (2015). Hydrocellular foam dressings promote wound healing associated with decrease in inflammation in rat periwound skin and granulation tissue, compared with hydrocolloid dressings. *Bioscience, Biotechnology, and Biochemistry, 79*(2), 185–189. https://doi.org/10.1080/09168451.2014.968088.

Zawadzki, J., & Kaczmarek, H. (2010). Thermal treatment of chitosan in various conditions. *Carbohydrate Polymers, 80*(2), 395–401. https://doi.org/10.1016/j.carbpol.

2009.11.037.

Zhang, S., Cheng, L., & Hu, J. (2003). NMR studies of water-borne polyurethanes. *Journal of Applied Polymer Science, 90*(1), 257–260. https://doi.org/10.1002/app.12696.

Zhang, S., Ren, Z., He, S., Zhu, Y., & Zhu, C. (2007). FTIR spectroscopic characterization of polyurethane-urea model hard segments (PUUMHS) based on three diamine chain extenders. *Spectrochimica Acta - Part A: Molecular and Biomolecular Spectroscopy, 66*(1), 188–193. https://doi.org/10.1016/j.saa.2006.02.041.

Zuber, M., Zia, K. M., Mahboob, S., Hassan, M., & Bhatti, I. A. (2010). Synthesis of chitin-bentonite clay based polyurethane bio-nanocomposites. *International Journal of Biological Macromolecules, 47*(2), 196–200. https://doi.org/10.1016/j.ijbiomac.2010.04.022.